Universal Scaling Relations in Molecular Superconductors

F. L. Pratt[1,*] and S. J. Blundell[2,†]

[1]*ISIS Facility, Rutherford Appleton Laboratory, Chilton, Oxfordshire OX11 0QX, United Kingdom*
[2]*Clarendon Laboratory, University of Oxford, Parks Road, Oxford OX1 3PU, United Kingdom*
(Received 22 October 2004; published 11 March 2005)

Scaling relations between the superconducting transition temperature T_c, the superfluid stiffness ρ_s, and the normal state conductivity $\sigma_0(T_c)$ are identified within the class of molecular superconductors. These new scaling properties hold as T_c varies over 2 orders of magnitude for materials with differing dimensionality and contrasting molecular structure and are dramatically different from the equivalent scaling properties observed for cuprate superconductors. These scaling relations place strong constraints on theories for molecular superconductivity.

DOI: 10.1103/PhysRevLett.94.097006 PACS numbers: 74.20.De, 74.25.Fy, 74.25.Nf, 76.75.+i

Understanding the phenomenon of superconductivity, now observed in quite disparate systems, such as metallic elements, cuprates, and molecular metals, involves searching for universal trends across different materials, which might provide pointers towards the underlying mechanisms. One such trend is the linear scaling between the superconducting transition temperature (T_c) and the superfluid stiffness ($\rho_s = c^2/\lambda^2$, where λ is the London penetration depth), first identified by Uemura *et al.* for the underdoped cuprates [1]. Recently, scaling relations between ρ_s and the normal state conductivity σ_0 have also been suggested and a linear relation between ρ_s and the product $\sigma_0(T_c)T_c$ was demonstrated by Homes *et al.* [2] for a set of cuprates and elemental superconductors (CES). Here we show that for molecular superconductors (MS) this linear scaling does not hold, but a different form of power-law scaling is found to link ρ_s, $\sigma_0(T_c)$, and T_c. These scaling properties hold as T_c varies over several orders of magnitude for materials with differing characteristic dimensionality and contrasting molecular structure. The scaling differs dramatically from that of the CES. Our findings have considerable implications for the theory of superconductivity in MS.

MS are generally regarded as members of the wider group of ‘‘exotic’’ superconductors that have attracted much research effort in recent years. A general feature of these exotic superconductors is the large carrier scattering rate observed in the normal state [3] leading to a picture of them as ‘‘bad metals’’ [4]. The scattering rate at temperatures near T_c may have particular relevance for the superconductivity, since it is expected that similar carrier interaction mechanisms would be dominant in the normal state resistance and in the pairing of carriers that leads to the formation of the superconducting state. It is therefore useful to study the correlation between $\sigma_0(T_c)$ and superconducting parameters such as T_c and ρ_s. Figure 1(a) shows ρ_s/c^2 ($= ne^2/m^*\epsilon_0 c^2$) and T_c derived from muon spin rotation (μSR) measurements in the vortex state [5,6], plotted against $\sigma_0(T_c)$ in the highest conductivity direction for a series of MS. The materials range from a highly anisotropic quasi-one-dimensional (q1D) organic superconductor [$(TMTSF)_2ClO_4$], through systems of two-dimensional (2D) layered organic superconductors (BETS and ET salts) to examples of three-dimensional (3D) fulleride superconductors; full details are listed in Table I [7–20]. Note that the parameter values vary over several orders of magnitude, which is important for successful determination of scaling properties. We find that ρ_s

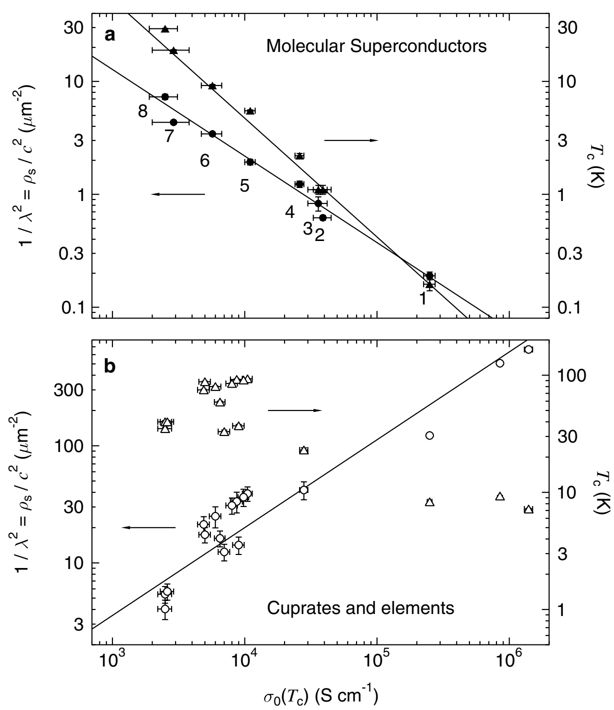

FIG. 1. (a) The inverse square of the penetration depth $1/\lambda^2$ (filled circles, left-hand scale) and T_c (filled triangles, right-hand scale) plotted against $\sigma_0(T_c)$ the normal state conductivity just above T_c in the most highly conducting direction for MS; the key is listed in Table I. (b) The CES data of Homes *et al.* [2] for comparison; $1/\lambda^2$ (open circles, left-hand scale) and T_c (open triangles, right-hand scale). Note the contrasting behavior of $1/\lambda^2$ compared to the MS.

TABLE I. Parameter values for the MS. Values for T_c and λ are derived simultaneously from μSR studies in the vortex state. λ corresponds to the estimated zero temperature value $\lambda(0)$. $\sigma_0(T_c)$ is the normal state conductivity in the most highly conducting direction. The conductivity is derived from reported multicontact resistance measurements in the case of the organics, single-domain scanning tunneling microscope measurements for K_3C_{60}, and far-infrared reflectivity for Rb_3C_{60}. Estimated uncertainties in the least significant digit are shown in brackets after each value. BETS stands for bis(ethylenedithio)tetraselenafulvalene, TMTSF stands for tetramethyltetraselenafulvalene, and ET stands for bis(ethylenedithio)tetrathiafulvalene.

Label	Material	T_c (K)	λ (μm)	$\sigma_0(T_c)$ (10^3 S cm^{-1})
1	κ-$BETS_2GaCl_4$	0.16(2) [7]	2.3(1) [7]	250(25) [13]
2	$(TMTSF)_2ClO_4$	1.1(1) [8]	1.27(3) [8]	39(6) (*a* axis) [14]
3	α-$ET_2NH_4Hg(SCN)_4$	1.1(1) [9]	1.1(1) [9]	36(6) [15]
4	β-ET_2IBr_2	2.2(1) [9]	0.90(3) [9]	26(2) [16]
5	λ-$BETS_2GaCl_4$	5.5(1) [7]	0.72(2) [7]	11(1) [17]
6	κ-$ET_2Cu(NCS)_2$	9.2(2) [9,10]	0.54(2) [9,10]	6(1) [18]
7	K_3C_{60}	18.9(1) [11]	0.48(2) [11]	2.9(9) [19]
8	Rb_3C_{60}	29.3(1) [12]	0.42(2) [12]	2.5(6) [20]

and T_c are related to $\sigma_0(T_c)$ by power laws of the form σ_0^m with $m = -1.05(3)$ for T_c and $m = -0.77(3)$ for ρ_s; in both cases there is a decrease in the strength of the superconducting property with increasing conductivity. For comparison, Fig. 1(b) shows a similar plot using the CES data of Homes *et al.* [2]. Here the overall trend for T_c is less clear and the trend for ρ_s shows a broad increase, opposite to that of the MS, with the positive exponent $m \sim 0.75$. This difference in the ρ_s-σ_0 scaling between CES and MS in the high conductivity direction contrasts with the reported similarity in scaling behavior between cuprates and organics in the low conductivity interplane direction [21]. That scaling on a ρ_s-σ_0 plot corresponds to $m = 0.85$, similar to the $m \sim 0.75$ seen for the cuprate high conductivity direction in Fig. 1(b). We thus have a situation in which the high and low conductivity directions in cuprates, along with the low conductivity direction in layered organics, all share a similar scaling property where ρ_s increases with increasing σ_0, whereas, for the high conductivity direction in the MS, ρ_s behaves quite differently in decreasing with increasing σ_0.

In the case of the MS, the different power laws seen for ρ_s and T_c against σ_0 in Fig. 1(a) imply that the scaling between them will not be of the linear Uemura form [1] but will follow another power law. Figure 2 shows the Uemura plot of T_c against $1/\lambda^2$ in log-log form where it can be seen that T_c follows ρ_s^m with the fitted value $m = 1.44(3)$. This approximate scaling of T_c with $\rho_s^{3/2}$, or equivalently λ^{-3}, in 2D organic MS was noted previously and discussed in terms of the 2D physics of layered superconductors [7,8,22,23]. However, it now appears that the scaling relations between T_c, ρ_s, and σ_0 are more universal, encompassing examples of q1D and 3D MS alongside the 2D systems. The nonlinear scaling between T_c and ρ_s in the molecular case is much harder to understand than the linear scaling seen in the cuprates. In the cuprates the carrier density n is directly controlled by the doping level; in the underdoped regime ρ_s is directly proportional to n and T_c has been suggested to be linked to ρ_s either through Bose-Einstein condensation of preformed pairs [24] or through a mechanism in which phase fluctuations of the superconducting order parameter determine T_c [25]. In contrast, for the MS, n is fixed by the unit cell size and stoichiometry of the crystal structure and varies only little across the range of materials, whose superconducting parameters are nevertheless varying across several orders of magnitude [23]. Differences in the superconducting properties must then arise entirely from differences in the details of the electronic many-body interactions.

Further evidence for fundamentally different behavior between molecular and nonmolecular superconductors is seen when an attempt is made to search for linear scaling between ρ_s and the product $\sigma_0(T_c)T_c$, of the form that was recently demonstrated by Homes *et al.* [2]. Figure 3(a) shows that such a simple linear scaling does not occur for the MS. The linear behavior seen for the nonmolecular

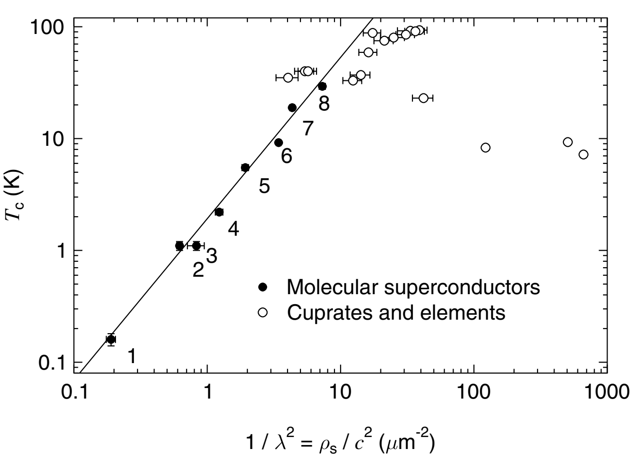

FIG. 2. Log-log Uemura plot of T_c against $1/\lambda^2$. Data for the CES tabulated by Homes *et al.* [2] are also shown for comparison. For the MS a scaling close to $\rho_s^{3/2}$ is observed, rather than the linear ρ_s scaling seen for the CES.

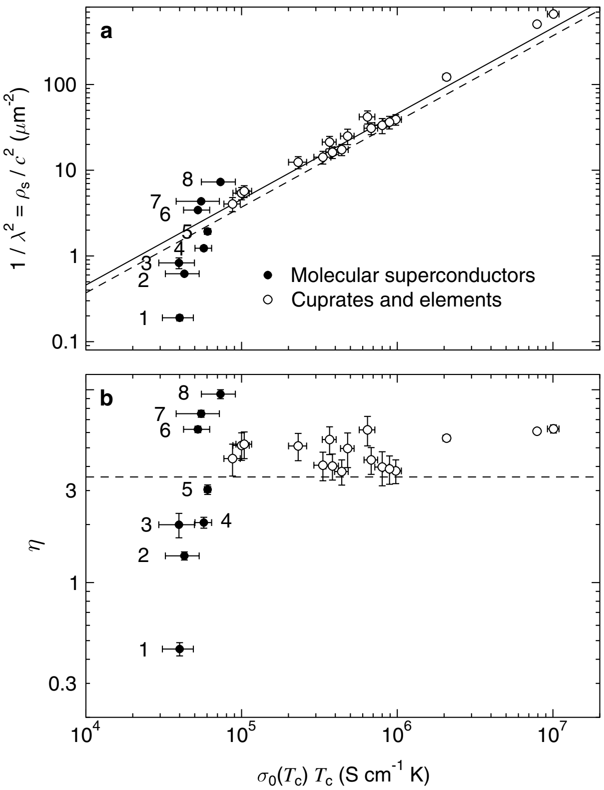

FIG. 3. (a) Plot of $1/\lambda^2$ against the product of T_c and $\sigma_0(T_c)$, following Homes *et al.* [2]. For the MS the data collapse onto a narrow ordinate range due to the inverse scaling between T_c and σ_0 demonstrated in Fig. 1(a). The open circles show the data of Homes *et al.* [2] along with the linear fit (solid line). The dashed line shows the scaling expected for a weak-coupling BCS superconductor in the high scattering rate limit (3). (b) The data expressed as an effective gap parameter (4). Whereas the CES data are grouped around a value of η just above the BCS limit (dashed line) and comparable to the gap ratios seen using other techniques, the MS points cover a wide range of η values, both above and below the BCS limit.

systems can be understood from applying the Ferrell-Glover-Tinkham sum rule for the real part of the frequency dependent conductivity [2,26],

$$\frac{2}{\pi}\int_0^\infty \sigma(\omega)d\omega = \frac{ne^2}{m^*} = \epsilon_0\rho_s, \quad (1)$$

where $\sigma(\omega)$ takes the Drude form $\sigma_0/[1 + (\omega/\Gamma)^2]$, with $\sigma_0 = ne^2/(m^*\Gamma)$ and Γ being the scattering rate. In the case where Γ is significantly smaller than the frequency corresponding to the superconducting energy gap $2\Delta/\hbar$, the whole free carrier spectrum is redistributed to zero frequency to give the superfluid response peak, i.e.,

$$\epsilon_0\rho_s = \sigma_0(T_c)\Gamma. \quad (2)$$

If, on the other hand, $2\Delta/\hbar$ is significantly smaller than Γ, then the normal state conductivity is independent of frequency in the gap region, i.e., $\sigma(\omega, T_c) = \sigma_0(T_c)$; in this case, as the superconducting gap forms, an area of the conductivity spectrum with frequency width $2\Delta/\hbar$ and height σ_0 is redistributed to zero frequency to give the superfluid response peak. This leads to the following expression for $\epsilon_0\rho_s$:

$$\epsilon_0\rho_s = \frac{2}{\pi}\sigma_0(T_c)\frac{2\Delta}{\hbar} = \frac{2k_B}{\pi\hbar}\eta\sigma_0(T_c)T_c, \quad (3)$$

where $\eta = 2\Delta/k_BT_c$. In Fig. 3(a) the dashed line shows (3) plotted taking the weak-coupling BCS limit $\eta = 3.53$ as a reference; this is seen to describe the general behavior of the CES data quite well. The effective value of η derived from the data assuming (3) is shown in Fig. 3(b), which reveals the considerable variation among the MS. Note that (3) was derived assuming that the ratio of carrier density to effective mass is the same in the normal and superconducting states. If, however, this assumption is relaxed, then the effective gap ratio observed in this plot becomes

$$\eta = \left(\frac{2\Delta}{k_BT_c}\right)\left(\frac{n_s}{m_s^*}\right)\Big/\left(\frac{n_n}{m_n^*}\right), \quad (4)$$

where the subscripts s and n refer to the superconducting and normal states, respectively. Strong coupling can increase η over the BCS value via the first term of (4), but the reduced values of η seen for many cases would require a contribution from at least one of the other two terms in (4), i.e., reduced carrier density and/or enhanced effective mass in the superconducting state.

Another way to look at the data is to plot the ratio $\epsilon_0\rho_s/\sigma_0$ which gives a measure of the effective frequency width Γ_e of the normal state conductivity spectrum that provides the superfluid response (Fig. 4). This will be determined either by Γ itself, following (2), or by $(2/\pi) \times (2\Delta/\hbar)$, following (3), whichever is smaller. For the CES the effective width follows the linear T_c dependence expected if it is proportional to either a BCS-type gap or a T-linear scattering rate. In contrast, for the MS, Γ_e follows a steeper power law T_c^α with the fitted value $\alpha = 1.58(5)$. This behavior suggests that the MS might actually be in the low-scattering-rate limit where $\Gamma < (2/\pi)2\Delta/\hbar$ and Γ_e follows Γ. We note that the fitted power law for Γ_e is also broadly consistent with the temperature dependence of the scattering rate deduced from the temperature dependent resistance of individual examples of the molecular metals; measurements for molecular metals just above T_c generally show power-law exponents in the region 1.5 to 2 [13–19].

From the scaling behavior of the MS highlighted here, the inverse relation between the strength of the superconducting properties and the normal state conductivity stands out as a characteristic feature of the MS, setting them apart from other classes of superconductor. The existence of such a clear scaling suggests that there are features of the electronic properties that are common across the MS, despite their differences in dimensionality and Fermi sur-

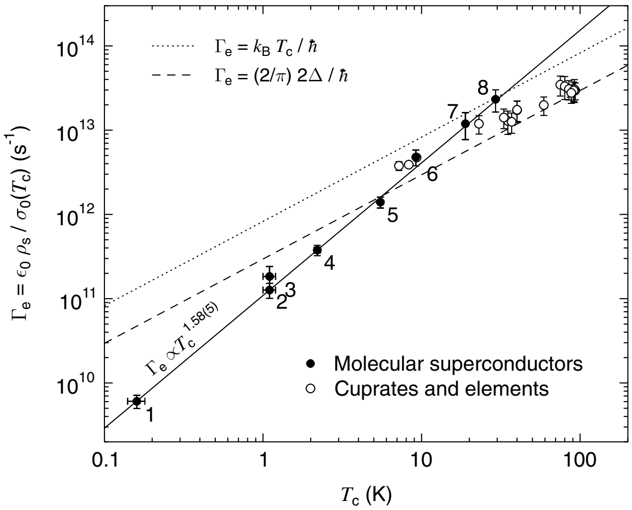

FIG. 4. Plot of ρ_s normalized by $\sigma_0(T_c)/\epsilon_0$ to give the frequency Γ_e. This reflects the effective width of the normal state conductivity spectrum, $\sigma(\omega)$, that has condensed into the superfluid peak at $\omega = 0$. For the CES, Γ_e appears to follow a linear temperature dependence. In contrast, for the MS the steeper temperature dependence $\Gamma_e \propto T_c^{1.58(5)}$ is seen (solid line). Γ_e for the CES and higher T_c MS is seen to lie between the BCS weak-coupling limit [dashed line (3)] and the Planckian scattering rate limit [3] (dotted line).

face topology. The simplicity of the scaling also suggests that it is being controlled by one dominant parameter, such as the ratio of the electron correlation energy on a molecule U to the electronic bandwidth W. U/W also controls the proximity of the Mott insulator (MI) phase; being close to the MI phase supports higher T_c and applied pressure can be used to tune U/W and pull the system away from the MI phase boundary. Depression of T_c by pressure is a property of the Bechgaard salts [27] and the fullerides [28]. In the κ-phase ET salts, it is found that pressure suppresses both T_c [29–31] and ρ_s [31] and enhances σ_0 [30]. However, standard approaches to modeling the crossover between the MI and the superconducting phase predict that the enhanced T_c near the MI phase is accompanied by a depressed ρ_s [32], exactly opposite to experiment. Identification of new theoretical models that match the observed scaling behavior is clearly necessary and finding such models should lead to significant progress in the understanding of MS.

We acknowledge discussions and interaction with Ben Powell, Ross McKenzie, Nikitas Gidopoulos, Steve Lee, Naoki Toyota, and Takahiko Sasaki. We are also grateful to Katherine Blundell for helpful comments on the manuscript and to the staff at the PSI and ISIS muon facilities for research support.

*Electronic address: f.pratt@isis.rl.ac.uk
†Electronic address: s.blundell@physics.ox.ac.uk

[1] Y. J. Uemura *et al.*, Phys. Rev. Lett. **62**, 2317 (1989).
[2] C. C. Homes *et al.*, Nature (London) **430**, 539 (2004).
[3] J. Zaanen, Nature (London) **430**, 512 (2004).
[4] V. J. Emery and S. A. Kivelson, Phys. Rev. Lett. **74**, 3253 (1995).
[5] S. J. Blundell, Contemp. Phys. **40**, 175 (1999).
[6] J. E. Sonier, J. H. Brewer, and R. F. Kiefl, Rev. Mod. Phys. **72**, 769 (2000).
[7] F. L. Pratt *et al.*, Polyhedron **22**, 2307 (2003).
[8] F. L. Pratt *et al.*, Synth. Met. (to be published).
[9] F. L. Pratt *et al.*, Physica (Amsterdam) **289B–290B**, 396 (2000).
[10] S. L. Lee *et al.*, Phys. Rev. Lett. **79**, 1563 (1997).
[11] Y. J. Uemura *et al.*, Nature (London) **352**, 605 (1991).
[12] R. F. Kiefl *et al.*, Phys. Rev. Lett. **70**, 3987 (1993).
[13] A. Kobayashi *et al.*, Chem. Lett. **1993**, 2179 (1993).
[14] K. Murata *et al.*, J. Phys. Soc. Jpn. **50**, 3529 (1981).
[15] H. Taniguchi, Y. Nakazawa, and K. Kanoda, Phys. Rev. B **57**, 3623 (1998).
[16] H. Bando *et al.*, J. Phys. Soc. Jpn. **54**, 4265 (1985).
[17] H. Tanaka *et al.*, J. Am. Chem. Soc. **121**, 760 (1999).
[18] H. Urayama *et al.*, Synth. Met. **27**, A393 (1988).
[19] S. Rogge, M. Durkut, and T. M. Klapwijk, Phys. Rev. B **67**, 033410 (2003).
[20] L. D. Rotter *et al.*, Nature (London) **355**, 532 (1992).
[21] S. V. Dordevic *et al.*, Phys. Rev. B **65**, 134511 (2002).
[22] F. L. Pratt *et al.* J. Phys. IV (France) **114**, 367 (2004).
[23] B. J. Powell and R. H. McKenzie, J. Phys. Condens. Matter **16**, L367 (2004).
[24] Y. J. Uemura, Physica (Amsterdam) **282C–287C**, 194 (1997).
[25] V. J. Emery and S. A. Kivelson, Nature (London) **374**, 434 (1995).
[26] R. A. Ferrell and R. E. Glover, Phys. Rev. **109**, 1398 (1958).
[27] K. Andres *et al.*, Phys. Rev. Lett. **45**, 1449 (1980).
[28] G. Sparn *et al.*, Phys. Rev. Lett. **68**, 1228 (1992).
[29] J. E. Schirber *et al.*, Phys. Rev. B **44**, 4666 (1991).
[30] J. Caulfield *et al.*, J. Phys. Condens. Matter **6**, 2911 (1994).
[31] M. I. Larkin *et al.*, Phys. Rev. B **64**, 144514 (2001).
[32] B. J. Powell and R. H. McKenzie, Phys. Rev. Lett. **94**, 047004 (2005).